MOLECULAR AND CELLULAR BIOLOGY, Jan. 1995, p. 505–516 Vol. 15, No. 1
0270-7306/95/$04.00+0
Copyright © 1995, American Society for Microbiology

Modulation of Cellular Thermoresistance and Actin Filament Stability Accompanies Phosphorylation-Induced Changes in the Oligomeric Structure of Heat Shock Protein 27

JOSÉE N. LAVOIE,[1] HERMAN LAMBERT,[1] EILEEN HICKEY,[2] LEE A. WEBER,[2] AND JACQUES LANDRY[1]*

Centre de recherche en cancérologie de l'Université Laval, L'Hôtel-Dieu de Québec, Québec, Québec G1R 2J6, Canada,[1] and Department of Biology, University of Nevada, Reno, Nevada 89557[2]

Received 30 March 1994/Returned for modification 4 May 1994/Accepted 11 October 1994

Phosphorylation of heat shock protein 27 (HSP27) can modulate actin filament dynamics in response to growth factors. During heat shock, HSP27 is phosphorylated at the same sites and by the same protein kinase as during mitogenic stimulation. This suggests that the same function of the protein may be activated during growth factor stimulation and the stress response. To determine the role of HSP27 phosphorylation in the heat shock response, several stable Chinese hamster cell lines that constitutively express various levels of the wild-type HSP27 (HU27 cells) or a nonphosphorylatable form of human HSP27 (HU27pm3 cells) were developed. In contrast to HU27 cells, which showed increased survival after heat shock, HU27pm3 cells showed only slightly enhanced survival. Evidence is presented that stabilization of microfilaments is a major target of the protective function of HSP27. In the HU27pm3 cells, the microfilaments were thermosensitized compared with those in the control cells, whereas wild-type HSP27 caused an increased stability of these structures in HU27 cells. HU27 but not HU27pm3 cells were highly resistant to cytochalasin D treatment compared with control cells. Moreover, in cells treated with cytochalasin D, wild-type HSP27 but not the phosphorylated form of HSP27 accelerated the reappearance of actin filaments. The mutations in human HSP27 had no effect on heat shock-induced change in solubility and cellular localization of the protein, indicating that phosphorylation was not involved in these processes. However, induction of HSP27 phosphorylation by stressing agents or mitogens caused a reduction in the multimeric size of the wild-type protein, an effect which was not observed with the mutant protein. We propose that early during stress, phosphorylation-induced conformational changes in the HSP27 oligomers regulate the activity of the protein at the level of microfilament dynamics, resulting in both enhanced stability and accelerated recovery of the filaments. The level of protection provided by HSP27 during heat shock may thus represent the contribution of better maintenance of actin filament integrity to overall cell survival.

Cells respond to environmental stress by the preferential synthesis and the accumulation of a conserved family of proteins, referred to as heat shock proteins (HSPs), and the acquisition of a dramatically increased capacity to survive subsequent hyperthermic stresses (28, 37, 44, 49). A cause-effect relationship between the accumulation of HSPs and thermotolerance has been established for some of these proteins. For example, gene transfection studies have shown that overexpression of HSP27 in mammalian cells is a sufficient condition for conferring thermoresistance (29, 35). Analyses of cell lines which constitutively overexpress various amounts of HSP27 or transiently express the protein after a selective induction revealed that cellular thermoresistance correlates with the amount of total HSP27 present at the time of heat shock. Within minutes of heat treatment, HSP27 is phosphorylated, shifts from a nonionic detergent-soluble to -insoluble cellular compartment, and relocalizes from the cytoplasm to within or around the nucleus (4, 5, 29–31, 35). It has been suggested that these modifications in HSP27 properties may be part of a mechanism that is initiated early during stress and activates the protective function of the protein.

Phosphorylation of HSP27 occurs rapidly following exposure to various stresses, but also, and most interestingly, it occurs in unstressed cells upon stimulation by serum or a variety of mitogens, cytokines, and inducers of differentiation (for a review, see reference 4). In quiescent cells stimulated by addition of serum, thrombin, or fibroblast growth factor, HSP27 is phosphorylated by a specific p45-54 serine protein kinase (19, 57). The assumption that HSP27 may exert phosphorylation-activated functions linked to growth-signaling pathways in unstressed cells was strongly supported by recent data which have shown that p45-54 HSP27 kinase can be activated in vitro by the p42-44 mitogen-activated protein kinases (19) and have suggested that HSP27 phosphorylation can regulate microfilament dynamics (36). Overexpression of human HSP27 in rodent cells enhances growth factor-induced F-actin accumulation following mitogenic stimulation of quiescent cells, whereas overexpression of a nonphosphorylatable HSP27 exerts a dominant negative effect and inhibits this response to mitogens. Moreover, an elevated level of HSP27 causes an increased concentration of F-actin at the cell cortex, where actin polymerization occurs, and an elevated pinocytotic activity, a property linked to increased actin filament dynamics. In contrast, cells overexpressing the nonphosphorylatable HSP27 show reduced cortical F-actin concentration and decreased pinocytosis activity relative to control cells (36). These results, together with others (9, 41, 42) which showed that HSP27 behaves in vitro as an actin-capping protein, suggested that HSP27 can function as a regulator of actin polymerization.

The nature of the protective function exerted by HSP27 in stressed cells is unknown, but several lines of evidence suggest

* Corresponding author. Mailing address: Centre de recherche en cancérologie de l'Université Laval, L'Hôtel-Dieu de Québec, 11, côte du Palais, Québec, Québec G1R 2J6, Canada. Phone: (418) 691-5555. Fax: (418) 691-5439. Electronic mail address: 2020053@saphir.ulaval.ca.

that it may be an extension of the normal phosphorylation-activated function of HSP27 at the level of actin filament. Phosphorylation of HSP27 during heat shock results from the activation of the same protein kinase and occurs at the same serine residues as in the case of mitogen-stimulated quiescent cells (19, 31, 57), suggesting that the normal function of the protein in signal transduction to microfilaments is likely to be activated in stressed cells also. Intriguingly, disruption of the cytoskeleton and disaggregation of actin fibers are among the most immediate effects of heat shock in higher eukaryotes (16, 20, 32, 56), and the stability of the actin filaments is considered an important factor in the survival of cells exposed to hyperthermia and other stresses (14, 40). Furthermore, elevated expression of HSP27 was shown to confer an increased stability of stress fibers during hyperthermia (35).

To ascertain the role of HSP27 phosphorylation in thermoprotection, we developed a family of clonal Chinese hamster CCL39 cell lines that constitutively express wild-type human HSP27 or equivalent amounts of a nonphosphorylatable mutant form of the protein. The data obtained from analyses of these cell lines showed that HSP27-mediated protection at the level of cellular survival and actin filament stabilization upon stress required activation of the protein by phosphorylation. We propose that phosphorylation-induced changes in HSP27 oligomeric structure modulate a stabilizing function of HSP27 at the level of actin filaments, resulting in better maintenance of actin organization and an enhanced survival rate after stress.

MATERIALS AND METHODS

Plasmids and cell lines. Plasmid pRSV-NEO contains the geneticin resistance gene (17); pKS2711 contains the wild-type human HSP27 gene (18); and pKSm15, pKSm78, pKSm82, pKSm83, pKSm7882, and pKSm157882 contain a human HSP27 gene in which the codons for Ser-15, Ser-78, Ser-82, and Ser-83 were converted to Gly codons individually or simultaneously, by site-directed mutagenesis as previously described (31). Cell lines were developed by transfecting the Chinese hamster CCL39 cell line (American Type Culture Collection) with 0.5 μg of pRSV-NEO and 35 μg of either an insert-free plasmid, pKS2711, pKSm157882, pKSm15, pKSm7882, or pKSm83, as previously described (29, 35, 36). Positive clones expressing different amounts of the transfected HSP27 were isolated from each group following selection with G418 (400 μg/ml) for 3 weeks. To eliminate possible clonal variability, four to six clones from each group were pooled to establish CCL39-neo control, HU27, HU27pm3, and HU27pm1-83 cell lines. In the nomenclature HU27pm*x-y*, HU27 stands for human HSP27, pm stands for phosphorylation mutant, *x* corresponds to the number of Ser residues converted to Gly, and *y* identifies the Ser residues converted. Cell lines were maintained and cell survival was estimated as previously described (29, 35, 36). Clonal cell lines were used at passage numbers lower than 25, and pools of clones were used at passage numbers lower than 10.

PAGE and immunodetection. For one-dimensional (1-D) sodium dodecyl sulfate-polyacrylamide gel electrophoresis (SDS-PAGE), proteins were extracted in SDS sample buffer (62.5 mM Tris-HCl [pH 6.8], 2.3% SDS, 10% glycerol, 5% β-mercaptoethanol, 0.005% bromophenol blue, 10 mM NaF, 1 mM phenylmethylsulfonyl fluoride [PMSF]) and fractionated through 10% polyacrylamide slab gels as described previously (29, 31). For 1-D isoelectric focusing (IEF)-PAGE, proteins were extracted in IEF lysis buffer (9.0 M urea, 2% 3-[(3-cholamidopropyl)dimethylammonio]-1-propanesulfonate [CHAPS], 2% amholines [75% Bio-lyte 5-7, 25% Bio-lyte 3-10], 5% β-mercaptoethanol, 10 mM NaF, 1 mM PMSF, 1 mM EDTA). IEF was carried out on rod gels as described previously (31, 57). For 2-D IEF SDS-PAGE, the IEF-gel rods were equilibrated in the SDS sample buffer for 20 min and then transferred to the top of the SDS-PAGE gels for the second dimension (29, 31). Gels containing ^{32}P-labeled samples were autoradiographed at −80°C with Dupont Lightning Plus intensifying screens. Unlabelled HSP27 proteins or isoforms were detected immunologically following transfer onto nitrocellulose membranes, and the relative amounts of HSP27 isoforms were measured by densitometric scanning of the autoradiograms. For pore exclusion limit electrophoresis on nondenaturing gels, proteins were extracted at 4°C in PELE sample buffer (20 mM Tris HCl [pH 7.4], 5 mM $MgCl_2$, 0.5% Triton X-100, 10 mM NaF, 1 mM dithiothreitol, 0.2 mM PMSF, 1 μM leupeptin, 1 μM pepstatin, 10% glycerol), vortexed for 30 s, and then centrifuged for 15 min at 12,000 × *g*. Aliquots of the supernatant were analyzed by pore exclusion limit electrophoresis on nondenaturing gels essentially as described previously (12), except that the polyacrylamide gradient used was 5 to 17% and electrophoresis was performed on a minigel apparatus (Bio-Rad). Native gels were run at equilibrium, usually for 16 h at 4°C. To transfer the native proteins, the gel was incubated for 20 min at 70°C in Tris-glycine buffer (25 mM Tris, 192 mM glycine [pH 8.3]) containing 0.25% SDS and then electroblotted in standard transfer buffer. Membranes were stained with a solution containing 0.2% Ponceau S in 5% trichloroacetic acid to visualize the protein markers (Pharmacia). Immunological detection was performed as previously described with Ha27Ab, a rabbit antiserum that was raised against Chinese hamster HSP27 and does not recognizes human HSP27 (29); anti-Ha (L2R3), a rabbit antiserum prepared against the carboxyl-terminal peptide AGKSEQS GAK of Chinese hamster and mouse HSP27 (this antibody does not react against human HSP27) (48); Hu27Ab, a rabbit antiserum that was raised against human HSP27 and does not react against Chinese hamster HSP27 (29); anti-HU71, a rabbit antiserum prepared against a carboxyl-terminal peptide of the human inducible HSP70 (50); and anti-HSP70, a rabbit antiserum raised against mouse HSP70 (43). ^{125}I-labeled goat anti-rabbit immunoglobulin G or horseradish peroxidase-linked goat anti-rabbit immunoglobulin G, revealed by the ECL detection system (Amersham), was used to detect the antigen-antibody complexes. Levels of proteins were determined by densitometric scanning of the autoradiograms. Absolute levels of human HSP27 were evaluated from a calibration curve made with standards containing known amounts of purified human HSP27.

Chromatographic analysis of HSP27. Cell extracts for size exclusion chromatography were prepared by nonionic-detergent lysis. Immediately following arsenite treatments, cells from a 175-cm^2 dish were scraped into 0.2 ml of TEPT buffer (10 mM Tris-HCl [pH 7.4], 1 mM EDTA, 10 mM NaF, 0.5% Triton X-100, 1 mM dithiothreitol, 0.2 mM PMSF, 1 μM pepstatin, 1 μM leupeptin). After the cell mixtures were vortexed, the supernatant was recovered following centrifugation at 12,000 × *g* for 15 min and then loaded onto a Superose 12 HR 10/30 column (Pharmacia), equilibrated in TEPG buffer (10 mM Tris-HCl [pH 7.4], 1 mM EDTA, 10% glycerol, 10 mM NaF, 0.1 mM PMSF, 1 mM dithiothreitol). Elution was done at a flow rate of 0.25 ml/min, and 0.5-ml fractions were analyzed on SDS-PAGE gels and by Western immunoblotting to determine the relative amount of HSP27 present in each fraction.

Cell fractionation analysis. For cell fractionation analysis, cells from a 25-cm^2 dish were lysed in TEPT extraction buffer. The protein extracts were vortexed and centrifuged at 4°C for 12 min at 12,000 × *g*. The pellets were resuspended in 1 volume of TEPT buffer. Equal amounts of supernatant (soluble fraction) and pellet (insoluble fraction) were analyzed by SDS-PAGE to determine the relative amount of HSP27 in each fraction or by 1-D IEF to determine the proportion of the various HSP27 isoforms.

Nondenaturing immunoprecipitation analysis. For nondenaturing immunoprecipitation analysis, cells from a 25-cm^2 dish were scraped into 1 ml of TEPT buffer. Extracts were vortexed and then centrifuged at 12,000 × *g* for 15 min at 4°C. All the following steps were done at 4°C. Undiluted Hu27Ab (100 μl) or Ha (L2R3) (50 μl) and 750 μl of 1% low-fat dry milk in TEBS buffer (10 mM Tris-HCl [pH 7.4], 1 mM EDTA, 10 mM NaF, 150 mM NaCl, 0.1 mM PMSF, 0.1% Triton X-100) were added to 450 μl of supernatant. The resulting mixture was incubated for 2 h. Protein A-Sepharose (Sigma 50% [vol/vol]) in TEBS buffer was then added at a concentration of 2 μl/μl of antibody, and the mixture was incubated for an additional 1 h. Samples were microcentrifuged for 30 s and washed three times with 1 volume of TEBS buffer. Immunoprecipitates were resuspended in 80 μl of SDS sample buffer without β-mercaptoethanol but containing 30 mM *N*-ethylmaleimide. A 20-μl volume was loaded on 1-D SDS-PAGE gel for analysis.

Immunofluorescence microscopy. Staining for HSP27 or F-actin for immunofluorescence microscopy was performed essentially as described previously (35, 36). Cells were plated on Lab-Tek polystyrene chamber slides (Life Technologies Inc.) for HSP27 localization or on fibronectin-coated glass slides for F-actin analyses. F-actin was detected with fluorescein isothiocyanate-conjugated phalloidin (33.3 μg/ml) diluted 1:50 in PBS (10 mM NaH_2PO_4, 130 mM NaCl, 2.7 mM KCl, 1 mM $MgCl_2$ [pH 7.5]). Hu27Ab and anti-Ha (L2R3) were used to detect human and hamster HSP27, respectively. The antibodies yielded only a low background staining in cells from heterologous species. HSP27 antigen-antibody complexes were detected with biotin-labeled anti-rabbit immunoglobulin G diluted 1:50 in phosphate-buffered saline (PBS) and revealed with Texas Red-conjugated streptavidin diluted 1:50 in PBS (Amersham). Confocal microscopy was performed with a Bio-Rad MRC-600 imaging system mounted on a Nikon Diaphot-TDM, equipped with a 60× objective lens with a 1.4 numerical aperture.

RESULTS

Phosphorylation is required for full thermoprotection mediated by HSP27. Human HSP27 is found in vivo as four major isoforms corresponding to nonphosphorylated (form A), monophosphorylated (B), biphosphorylated (C), and triphosphorylated (D) HSP27. Two of the three major phosphorylation sites of human HSP27 have been identified biochemically as Ser-78 and Ser-82 and shown to be targets of phosphorylation in vivo (31). The third major phosphorylation site is

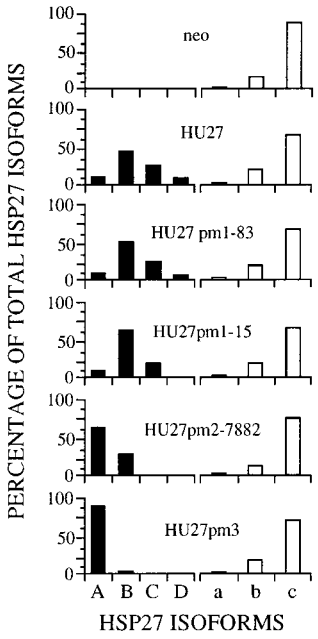

FIG. 1. In vivo phosphorylation of mutant forms of human HSP27. Control Chinese hamster cell lines (*neo*) or clones expressing wild type (HU27) or the mutant forms involving the changes Ser-83 → Gly (HU27pm1-83), Ser-15 → Gly (HU27pm1-15), Ser-15 and Ser-78 → Gly (HU27pm2-7882), or Ser-15, Ser-78, and Ser-82 → Gly (HU27pm3) were incubated in the presence of 200 μM sodium arsenite for 1 h at 37°C to induce maximal phosphorylation of HSP27. Total-cell proteins were extracted in IEF buffer immediately after treatment and were fractionated by 1-D IEF-PAGE. Endogenous Chinese hamster and exogenous human HSP27 isoforms were detected by Western blot analyses with specific antisera against hamster and human HSP27, respectively. The relative amounts of the four human HSP27 isoforms (A, B, C, and D), as well as the three Chinese hamster HSP27 isoforms (a, b, and c) in each cell line were determined by densitometric scanning of the autoradiograms. The results are presented as the percentage of each isoform relative to the total amount of the protein. Solid bars, human HSP27; open bars, Chinese hamster HSP27.

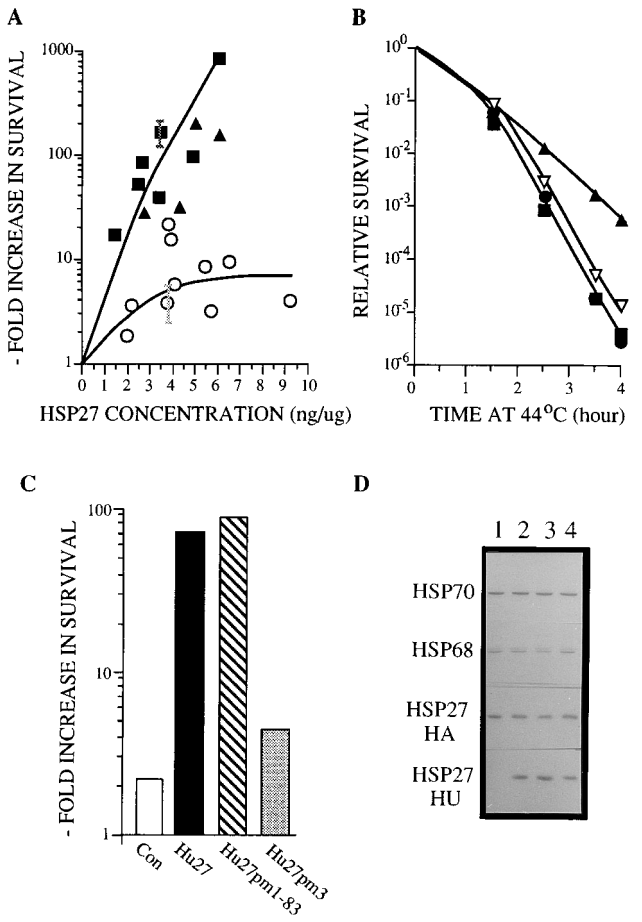

FIG. 2. Phosphorylation is required for HSP27-mediated thermoprotection. Families of Chinese hamster cell lines that express different levels of the human HSP27 (HU27 cells) or the nonphosphorylatable human HSP27 (HU27pm3 cells) were developed. (A) The various clonal cell lines were heat shocked for 4 h at 44°C and plated at appropriate concentrations to determine their capacity to form colonies at 37°C; this was compared with the thermoresistance of control cells expressing the *neo* gene only. The results are expressed as the fold increase in survival of the cell lines relative to similarly heat-shocked control *neo* cells as a function of the HSP27 concentration in the cells. The error bars represent the standard deviation in seven distinct experiments in which survival of HU27 clone 6 cells and HU27pm3 clone V cells was evaluated. Symbols: ■, HU27 clones; ▲, HU27pm1-83 clones; ○, HU27pm3 clones. (B) Control untransfected CCL39 (■), *neo* cells (clone 3) (●), HU27 cells (clone 6) (▲), and HU27pm3 cells (clone V) (▽) were heat shocked at 44°C for the indicated periods, and cell survival was determined by measuring colony formation. (C) Clones containing equivalent amounts of wild-type or mutant human HSP27 were pooled separately to eliminate possible clonal variabilities. Cultures of pools were exposed to 44°C for 4 h and then plated at appropriate densities for colony formation at 37°C (Con, *neo* cells). (D) Western blot evaluation of the levels of HSP70, HSP68, and Chinese hamster and human HSP27 in the various cell lines used in panel C. Lanes: 1, *neo* cells; 2, HU27 cells; 3, HU27pm1-83 cells; 4, HU27pm3 cells.

thought to be Ser-15 on the basis of sequence homology with the mouse protein and the presence of a conserved HSP27 kinase recognition sequence motif RXXS at this site (15, 31). To confirm that human HSP27 is phosphorylated at Ser-15 in vivo, Chinese hamster cell lines expressing either the wild-type human HSP27 or various forms of human HSP27 with Ser-15 and/or Ser-78 and Ser-82 replaced with Gly (see below for the development of the cell lines) were treated with sodium arsenite to induce maximal phosphorylation of HSP27. The phosphorylation of each mutant HSP27 protein was analyzed and compared with the phosphorylation of wild-type human HSP27, a control mutant with a Ser-83 → Gly mutation, and the endogenous Chinese hamster protein. As expected, the wild-type human HSP27 and the control mutant were expressed as three major phosphorylated isoforms (B, C, and D) in arsenite-treated Chinese hamster cells, whereas the endogenous Chinese hamster HSP27 was present as two major phosphorylated isoforms, b and c (Fig. 1). Chinese hamster HSP27, like mouse HSP27, lacks Ser-78 (human sequence) and has only two phosphorylation sites (15, 34). HSP27 with both Ser-78 and Ser-82 replaced by Gly was phosphorylated at a much lower rate than the wild-type protein and produced only the monophosphorylated isoform B. The Ser-15 → Gly replacement alone caused no major reduction in the phosphorylation rate. However, this protein mutant accumulated as mono- and biphosphorylated HSP27 and no triphosphorylated protein could be detected. As expected, the triple mutant protein with mutations at Ser-15, Ser-78, and Ser-82 was not phosphorylated significantly.

To determine the role of phosphorylation in the thermoprotective function of HSP27, families of clonal Chinese hamster CCL39 cell lines that express different levels of wild-type human HSP27 or equivalent amounts of the nonphosphorylatable triple-mutant HSP27 were developed. Control cell lines expressing the Ser-83 → Gly mutant HSP27 or the marker gene *neo* only were also produced. Each individual cell line (6 to 10 lines per family) was heat shocked for 3.5 h (data not shown) or 4 h (Fig. 2A) at 44°C and then plated at the appropriate

concentration at 37°C to determine survival from the percentage of cells capable of forming colonies. Duplicate cultures were prepared for each of the various cell lines to monitor human HSP27 concentration by Western blot analysis. The thermoresistance of cells overexpressing either the wild-type human HSP27 or the control mutant HSP27 increased proportionally to the amount of expressed human HSP27. After heat shock, the survival of clones expressing 6 ng of wild-type human protein per μg of total protein was increased by about 1,000-fold relative to *neo* cells or untransfected cells. Such increase in thermoresistance should be compared with the 3,000-fold increase in survival obtained with untransfected CCL39 cells after treatments that induce the full spectrum of heat shock proteins and an increase of about 10 ng of endogenous HSP27 per μg of total protein (data not shown). In contrast, clones overexpressing the nonphosphorylatable form of HSP27 were only slightly protected, even at the highest concentration of the protein. The relative survival was increased only ~sevenfold at a level of 6 ng of the nonphosphorylatable HSP27 per μg of total protein and did not increase further even in cells expressing 9 ng of mutant HSP27 per μg. The thermoresistance of two clonal cell lines expressing the same levels (~3.5 ng/μg) of the wild-type and nonphosphorylatable human proteins, respectively, was further analyzed and compared with that of *neo* and untransfected cells. As shown in Fig. 2B, incubation at 44°C for increasing periods caused a gradual decrease in the survival of all cell lines. Wild-type HSP27, but not the nonphosphorylatable HSP27, caused a reduction in the rate of cell killing. The effect became significant after 1.5 h of treatment.

Cellular thermoresistance in pools made with clonal cells from each family that expressed between 3 and 4 ng of exogenous HSP27 was also evaluated. The survival of HU27, HU27pm3, and HU27pm1-83 cells was compared with that of a pool of clones expressing the marker gene only. As observed in individual clones, the substitution of the three phosphorylatable serines rendered HSP27 much less efficient in protecting the cells. In contrast, the substitution at Ser-83 did not affect the efficiency of HSP27 as a thermoprotective molecule (Fig. 2C).

In addition to monitoring the level of the human proteins, we investigated all the cell lines and pools of cell lines used in this study to ensure that expression of endogenous heat shock proteins was not affected by the presence of the exogenous HSP27. Western blot analyses with antibodies specific for the Chinese hamster HSP27, HSP70, and the inducible HSP70 (HSP68) revealed no alteration in the expression of these proteins in any of the clonal cell lines (data not shown) or pools of these cells (Fig. 2D). Moreover, endogenous Chinese hamster HSP27, as well as the inducible HSP70, accumulates in these cells in response to heat shock to the same extent as in untransfected cells (data not shown). In addition, we examined the effect in several cell lines of expressing high levels of the nonphosphorylatable human protein on the phosphorylation of the endogenous HSP27 in response to heat shock or arsenite. As illustrated in Fig. 1 for one representative clone of each family, the endogenous HSP27 was phosphorylated to the same level in HU27pm3 cells as in HU27 cells after treatment with sodium arsenite for 1 h. The transfected proteins also had no effect on the uninduced level of phosphorylation of the endogenous proteins. This was confirmed in an extensive analysis with several cell lines expressing different levels of the wild-type or mutant HSP27 (data not shown). The results indicated that expression of the human proteins did not generate a detectable stress response in the host cells.

Phosphorylation of HSP27 modulates the microfilament response to heat shock and the protection from cytochalasin D-induced disruption of actin filaments, growth inhibition, and cell killing. We previously showed that a selective induction of Chinese hamster HSP27 in mouse NIH 3T3 cells caused an increased stability of F-actin structures during heat shock (35). A similar protective role at the level of actin filaments was suggested for the HSP27 homolog αB-crystallin (21). To determine the role of HSP27 phosphorylation in this protection, we investigated the effect of heat shock on the integrity of actin filaments in a representative clonal cell line of HU27pm3 cells (clone V, 3.7 ng/μg) compared with HU27 cells (clone 6, 3.4 ng/μg) and control *neo* cells (clone 3). In the three cell types, heat shock caused a rapid disruption of the fine structure of the actin filaments at the cell cortex and of the actin fibers in the cytoplasm. This resulted in a loss of membrane protrusions and retraction of the cells from the substratum. Notable differences in the severity of the effects were, however, observed between the cell lines.

In HU27pm3 cells, which expressed the nonphosphorylatable form of HSP27, both the cortical and fiber structures of F-actin were totally disorganized, leaving only a punctate cytoplasmic staining which often concentrated under the cell membrane. As a result of these alterations, the cells became rounded, possibly because of a contraction of the remaining F-actin and a reduced adherence to substratum (Fig. 3F). In comparison, a net protection of the cytoskeleton was observed in HU27 cells overexpressing the wild-type human HSP27 (Fig. 3E). In these cells, the effect of heat shock was still quite severe; however, a large proportion of the cells kept long, extended filament cables and membrane protrusions containing fine actin fibers. Levels of damage intermediate between those of HU27 and HU27pm3 cells were seen in the control *neo* cells. In contrast to HU27pm3 cells, some filament cables were still visible in *neo* cells after heat shock but in a lesser amount and in fewer cells than in HU27 cells. Also, heated *neo* cells remained more spread on the substratum than did HU27pm3 cells but showed fewer membrane protrusions and submembranous actin filaments than HU27 cells.

The apparent higher and reduced stability of actin filaments during heat shock in cells overexpressing HSP27 and mutant HSP27, respectively, may be related to the proposed phosphorylation-activated function of the protein at the level of F-actin dynamics. It was shown that accumulation of F-actin in quiescent Chinese hamster fibroblasts stimulated by mitogens is enhanced in cells overexpressing HSP27 and inhibited in cells expressing the nonphosphorylatable protein (36). A similar function activated in exponentially growing cells subjected to stressing conditions may help preserve filament integrity. To address this possibility more directly, we investigated the effect of cytochalasin D on the microfilaments of clones from control, HU27, and HU27pm3 cells. Cytochalasin D is known to be a highly specific inhibitor of actin polymerization. Inhibition occurs mainly because cytochalasin D binds with high affinity to the fast-growing ends of actin filaments, thereby preventing addition of monomers (27, 46). As expected, inhibiting actin polymerization by a 1-h exposure to 0.5 μM cytochalasin D caused major disturbances in the F-actin staining patterns and a reduction in the size and number of the actin fibers in all three cell types (Fig. 4A to F). However, a net difference was observed in the effect of the drug on control and HU27pm3 cells compared with HU27 cells. Examination of some 300 individual cells from each cell type indicated that 45% of the HU27 cells retained short and thin but still discernible actin fibers after the treatment, as compared with 20% in both the control and the mutant cell lines (reference 35 and data not

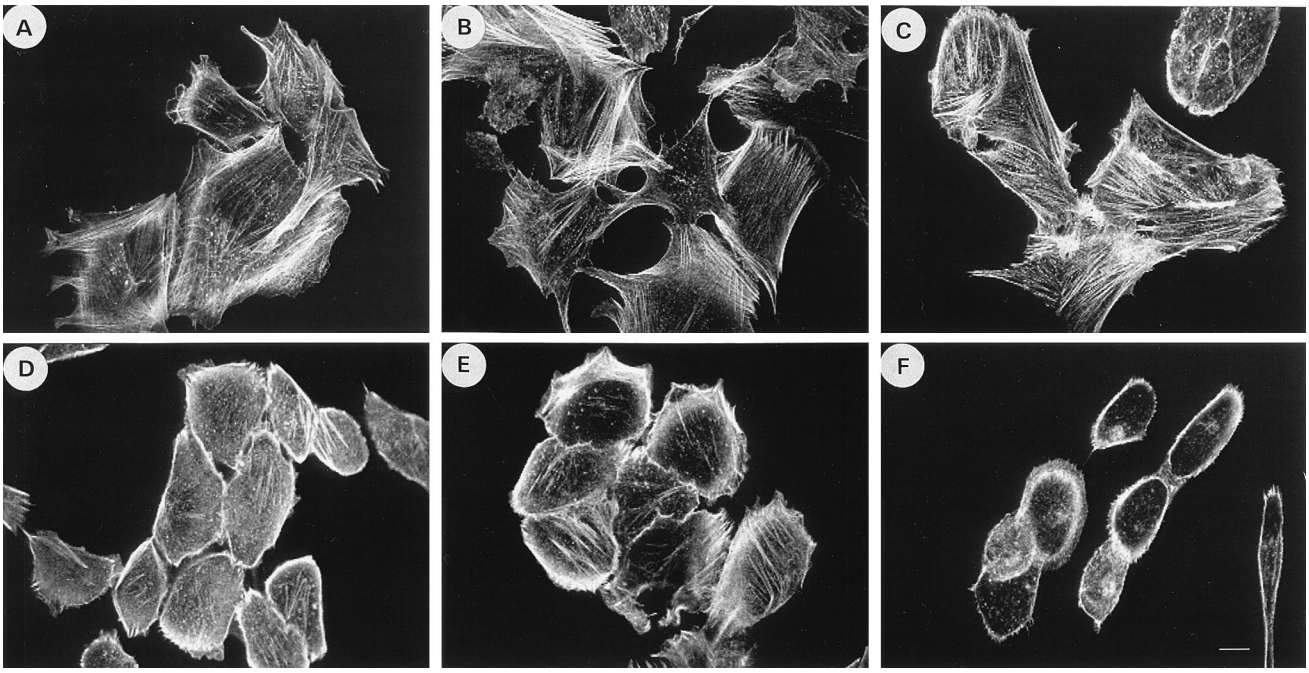

FIG. 3. Phosphorylation is required for HSP27-mediated protection of cell shape and microfilament integrity during heat shock. *neo* (clone 3) (A and D), HU27 (clone 6) (B and E) and HU27pm3 (clone V) (C and F) cells were plated on fibronectin-coated glass slides, allowed to attach for 16 h, and then left untreated (A to C) or heat shocked for 30 min at 44°C (D to F). Immediately after this, F-actin was stained with fluorescein isothiocyanate-conjugated phalloidin and the microfilaments were visualized by confocal microscopy. The confocal aperture was adjusted to obtain maximum resolution of F-actin and kept constant for all specimen analysis. Bar, 10 μm.

shown). In both control and HU27pm3 cells, most of the F-actin remaining after the treatment was found in small granular structures, yielding an irregular punctate staining (Fig. 4D and F). In the most severely affected cells, F-actin was found further aggregated, forming typical heavily stained actin patches (e.g., Fig. 4F). As a likely consequence of this disorganization of F-actin, the cells retracted from the substratum and became more rounded. In contrast, the punctate F-actin staining was seldom seen in similarly treated HU27 cells (Fig. 4E). A higher proportion of these cells retained a flat morphology and extended membrane structures, suggesting an overall maintenance of the cortical microfilament organization. An even more striking difference between control, HU27pm3, and HU27 cells was observed during the recovery period after removal of the drug (Fig. 4G to I). Control *neo* cells totally recovered their pretreatment level of F-actin and regained normal cell morphology by 1 h in the absence of the drug (Fig. 4G). HU27 cells recovered faster. After an identical recovery period, a much more intense F-actin staining was observed in these cells than in *neo* cells; the level of staining even surpassed that seen before the treatment (Fig. 4H). Remarkably, recovery of HU27pm3 cells was very similar to that of control cells, suggesting again that the nonphosphorylatable protein was not active (Fig. 4I).

To determine whether HSP27-mediated stabilization of actin could provide a significant advantage at the whole-cell survival level during stress and account for the increased thermoresistance of HSP27-overexpressing cells, we assessed the effect of the phosphorylatable and the nonphosphorylatable HSP27 on improving the growth and survival of cells subjected to chronic exposure to cytochalasin D. In the absence of cytochalasin D, wild-type and nonphosphorylatable HSP27 had no significant effect on growth rates (Fig. 5A). The three cell lines grew with a doubling time of approximately 15 h. HSP27 provided a clear protection in the presence of 0.5 μM cytochalasin D. Under these conditions, growth of the *neo* and HU27pm3 cells was almost totally inhibited, whereas the doubling time of HU27 cells was at about 21 h (Fig. 5B). A similar protective effect of HSP27 was observed at the level of colony formation. At all concentrations tested, a marked reduction in toxicity was observed in HU27 cells, whereas HU27pm3 cells were as sensitive as control *neo* cells (Fig. 5C). Notably, the plating efficiency of HU27 cells in the presence of 0.1 μM cytochalasin D was reproducibly increased compared with that of untreated cells. At this low nontoxic concentration, cytochalasin D may promote cell attachment and colony formation by stimulating the function of HSP27 at the level of actin filament dynamics. Consistent with this hypothesis, cytochalasin D treatment caused a small but reproducible increase in the phosphorylated b and c isoforms of HSP27 (Fig. 5D).

HSP27 relocalization following heat shock is not mediated by phosphorylation. Representative clones expressing the wild-type or the nonphosphorylatable human HSP27 and a control *neo* cell line were used to assess the importance of phosphorylation on the heat-induced intracellular translocation of the protein (Fig. 6). Cultures were heat shocked at 44°C, processed immediately for endogenous and human HSP27 immunolabelling, and analyzed by immunofluorescence confocal microscopy. As shown previously (36), Chinese hamster HSP27 in unstressed cells has a general cytoplasmic distribution with an enhanced concentration in motile membrane protrusions such as ruffles and lamellipodia (Fig. 6A). A 20-min treatment which was sufficient to induce strong phosphorylation of HSP27 (see Fig. 7C) caused no change in the distribution of the protein (data not shown). After 1.5 h at 44°C, motile HSP27-containing structures such as ruffles were no longer observed and the endogenous protein became concentrated in perinuclear structures (Fig. 6D). By confocal microscopy, we

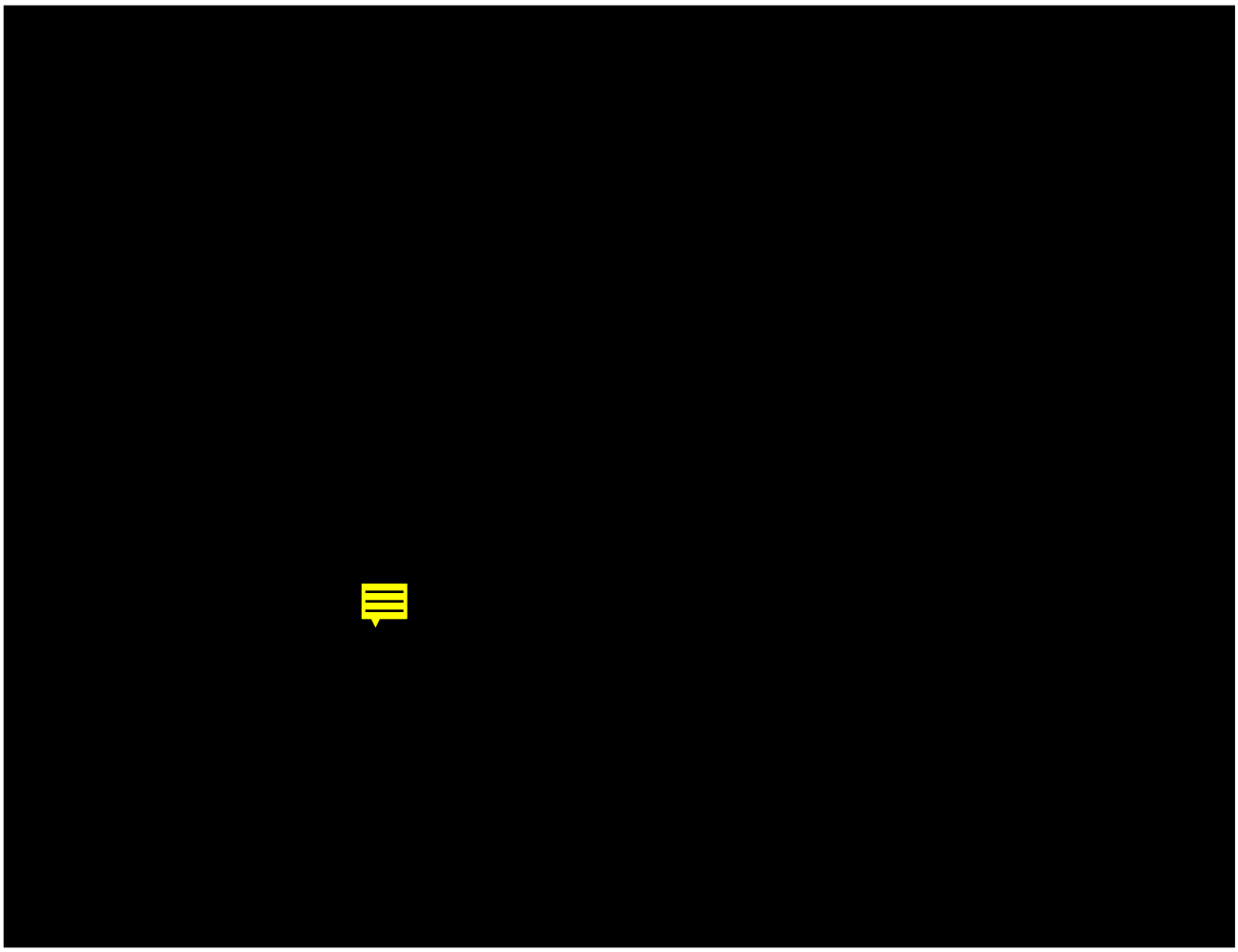

FIG. 4. Phosphorylation of HSP27 modulates the response of microfilaments to cytochalasin D treatments. *neo* (clone 3) (A, D and G), HU27 (clone 6) (B, E and H) and Hu27pm3 (clone V) (C, F and I) cells were plated on fibronectin-coated glass slides, allowed to attach for 16 h, and then left untreated (A to C) or incubated in the presence of 0.5 μM cytochalasin D for 1 h (D to I). Immediately after cytochalasin D treatment (D to F) or 1 h after removal of the drug (G to I), the cells were processed for F-actin staining with fluorescein isothiocyanate-conjugated phalloidin. The confocal aperture was adjusted to obtain maximum resolution of total F-actin and kept constant during all specimen analysis. Confocal pseudo-color images were used to quantitatively illustrate F-actin levels in the cells. The color bar shows the correspondence between fluorescence intensity and color. Scale bar, 10 μm.

never observed a nuclear relocalization of HSP27 after heat shock in CCL39 cells. This suggested that the nuclear relocalization of HSP27 previously observed in other cell lines (4, 5, 35) may be cell type specific. Similar analyses performed with HU27 and HU27pm3 cells indicated that the wild-type and mutant human proteins localized in a manner identical to the endogenous protein in both control and heat-shocked cells (Fig. 6B to D and F). Moreover, overexpression of the foreign proteins had no detectable effect on the distribution of the endogenous protein before and after heat shock (data not shown). In addition to showing that the mutant protein localized normally in the cells, these observations indicated that phosphorylation is not essential to trigger the relocalization of HSP27.

HSP27 insolubilization following heat shock is not mediated by phosphorylation. Heat shock is also known to induce a partial insolubilization of HSP27, causing a shift of the protein from a nonionic detergent soluble fraction to an insoluble fraction (4, 5). We next examined the role of phosphorylation on this process. In cells maintained at 37°C, more than 95% of either the endogenous, the wild-type human, or the nonphosphorylatable HSP27 was recovered in the soluble fraction (Fig. 7A and B). The three protein species were insolubilized at the same rate at elevated temperatures. After 20 min at 44°C, between 30 and 40% of the wild-type HSP27 and the triple-mutant human HSP27, as well as the endogenous Chinese hamster HSP27, were insoluble; after 2 h, 80% were insoluble. Additional evidence that phosphorylation had no effect on the rate of insolubilization of the proteins was obtained by comparing the phosphorylation levels of the Chinese hamster HSP27 in the Triton-soluble and Triton-insoluble fractions. Again, no strict correlation between the phosphorylation and insolubilization was observed (Fig. 7C). In contrast to insolubilization, which increased continuously during the first 2 h of heat shock, phosphorylation of HSP27 in both the soluble and insoluble fractions was already at maximal value after 15 to 20 min of heat treatment and was maintained at this level for up to 1 h. Phosphorylation decreased during incubation for periods longer than 1 h at 44°C, whereas insolubilization was maintained at high level. Furthermore, there was no systematic enrichment of phosphorylated species in either the soluble or insoluble fractions at any time during this period.

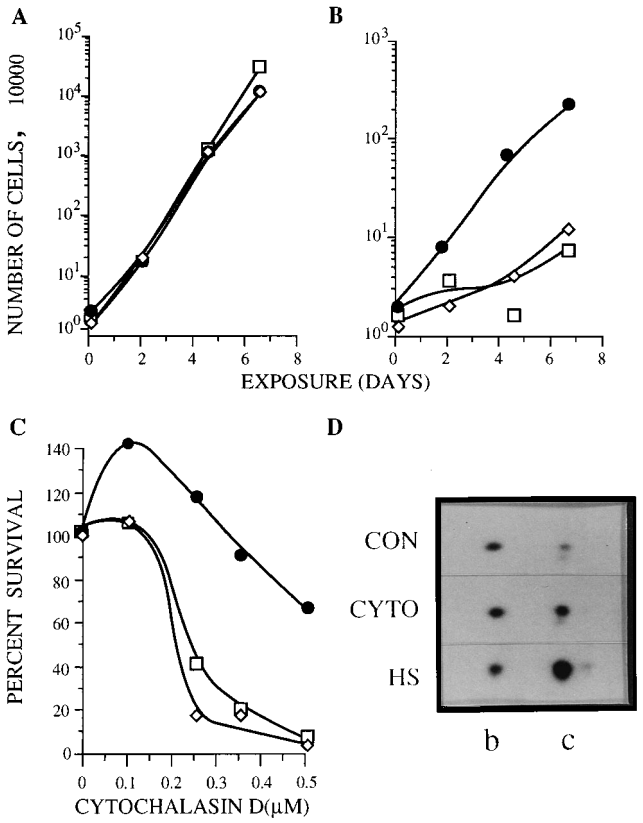

FIG. 5. HSP27 but not mutant HSP27 expression protects against cytochalasin D-induced growth inhibition and cell killing. Pools of control *neo* (□), HU27 (●), and HU27pm3 (◇) clones were plated at appropriate densities and incubated in the presence of cytochalasin D. (A and B) Cell growth in the absence (A) or the presence (B) of 0.5 μM cytochalasin D was measured by counting the cells at intervals during the first 7 days. (C) Relative survival of cells incubated in the presence of different concentrations of cytochalasin D was determined by counting the number of colonies after 10 days. (D) Effect of cytochalasin D on the incorporation of ^{32}P into Chinese hamster HSP27 isoforms b and c. *neo* cells were incubated for 2 h in the presence of $^{32}PO_4^{3-}$ and then left untreated (CON), incubated for 1 h with 0.5 μM cytochalasin D (CYTO), or heat shocked for 20 min at 44°C (HS). Proteins were extracted and analyzed by 2-D PAGE. Only the portion of the autoradiograms including HSP27 isoforms b and c is shown.

Intriguingly, even though the Chinese hamster HSP27 was insolubilized at the same rate as the human proteins in the transfected cells, we found that Chinese hamster HSP27 insolubilized at a higher rate in control cells than in either transfected-cell type (Fig. 7B). In control untransfected CCL39 cells, 60% of the Chinese hamster HSP27 proteins were insoluble after 20 min of heat treatment compared with 30% in human HSP27-expressing cells. These results implied that some phosphorylation-independent properties of human HSP27 contributed to protection of the endogenous HSP27 from insolubilization. One possibility is that the in vitro chaperonin function of HSP27 is phosphorylation independent (22, 39). Another possibility is that the human protein is intrinsically more heat resistant than the hamster protein. HSP27, like the homologous lenticular α-crystallin proteins, is known to form oligomeric structures both in vivo and in vitro (4, 5, 8). Under these conditions, mixed oligomers of human and hamster HSP27 might be expected to be more resistant than homotypic oligomers of hamster HSP27 to thermal denaturation and thus to heat-induced insolubilization.

Induction of HSP27 phosphorylation is accompanied by a change in its oligomeric organization. To examine the putative association of the human and Chinese hamster proteins, quantitative nondenaturing immunoprecipitations followed by immunodetections were performed in HU27, HU27pm3, and *neo* clonal cell lines with specific antibodies against human or Chinese hamster HSP27 (Fig. 8). Both antibodies were highly specific: no Chinese hamster HSP27 was detected with the anti-Ha (L2R3) antibody after immunoprecipitation of extracts from *neo* cells, containing only Chinese hamster HSP27, with Hu27AB or immunoprecipitation of extracts from HeLa cells, containing only human HSP27, with anti-Ha (L2R3) or Hu27Ab (Fig. 8, lanes 1 to 3). In unstressed HU27 and HU27pm3 cells, Hu27Ab was as efficient as anti-Ha (L2R3) in precipitating the endogenous Chinese hamster HSP27 (lanes 5, 7, 9, and 11), and the amount precipitated was equal to the amount obtained following immunoprecipitation of Chinese hamster HSP27 in *neo* cells with anti-Ha (L2R3) (compare lane 4 with lanes 5 and 7). This suggested that the endogenous Chinese hamster HSP27 was entirely associated with human HSP27 in HU27 and HU27pm3 cells. The same analysis was repeated in cells in which HSP27 phosphorylation was induced by incubation with sodium arsenite. Sodium arsenite was chosen in this experiment because it induces strong phosphorylation yet causes minimal insolubilization of HSP27 compared with heat shock. Hu27Ab was much less efficient at immunoprecipitation of the endogenous Chinese hamster HSP27 in stressed cells than in unstressed cells. Arsenite treatment caused a 75 and 60% reduction in the amount of Chinese hamster proteins immunoprecipitated by Hu27Ab in stressed HU27 and HU27pm3 cells, respectively (lanes 6 and 8), whereas it had no effect on the amount of human HSP27 immunoprecipitated by Hu27Ab (lanes 13 to 16) or on the amount of Chinese hamster protein precipitated by anti-Ha (L2R3) (lanes 9 to 12). These results indicated that phosphorylation reduced the heterologous association of the proteins, implying that phosphorylation caused some modifications in the structure of the HSP27 oligomers.

The oligomeric status of HSP27 was investigated more directly by estimating its apparent native molecular weight by pore exclusion limit electrophoresis. In control untransfected Chinese hamster cells, the HSP27 oligomeric structure was highly dynamic and the protein exhibited different molecular weights depending on the experimental conditions (Fig. 9). In unstressed exponentially growing cells, all HSP27 was detected in two major forms of 200 and 250 kDa (Fig. 9, lanes 1, 4, and 9). Phosphorylation of the protein induced by incubation of the cells with sodium arsenite caused a drastic reduction in the size of the structures. The 200- and 250-kDa complexes totally disappeared and were replaced by a 125-kDa structure (lanes 2, 8, and 12). After heat shock, most HSP27 became insoluble and thus could not be analyzed; however, the HSP27 particles that remained soluble were also reduced in size to about 150 kDa (lane 3). A modification in the size of the HSP27 structures was also observed during exit of the cell cycle upon serum deprivation and during restimulation of the cells by addition of serum or thrombin, which are full mitogens in these cells and induce the phosphorylation of HSP27 (11, 57). Serum deprivation led to an enlargement of some of the HSP27 species to ~600 kDa (lane 5). Within 15 min after mitogenic stimulation, the 600-kDa species dissociated and new discrete bands appeared at 150 and 125 kDa (lanes 6 and 7).

A redistribution of HSP27 oligomers to lower-molecular-weight species was thus observed following all treatments that induce HSP27 phosphorylation. Moreover, the diminution in the size of HSP27 complexes appeared to be proportional to the degree of HSP27 phosphorylation. Maximal phosphoryla-

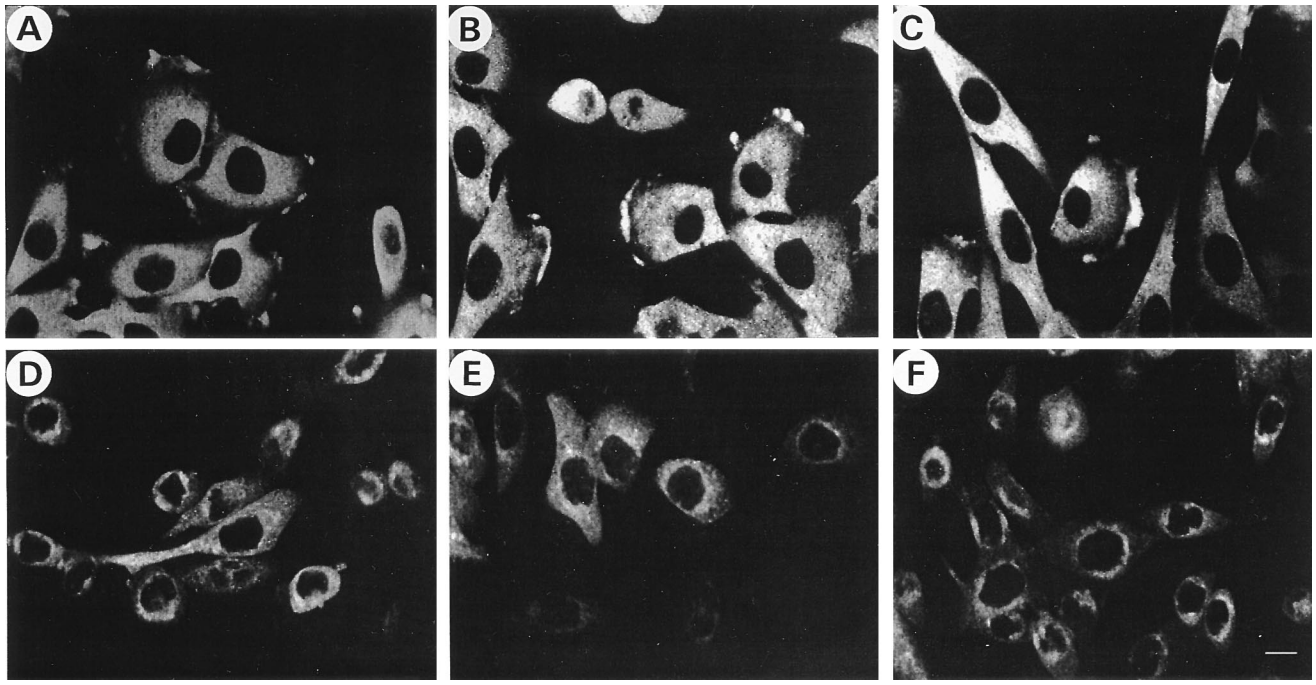

FIG. 6. Intracellular localization of HSP27 and mutant HSP27 in control and heat-shocked cells. Cells were plated on Lab-Tek polystyrene chamber slides and grown for 16 h. Indirect confocal immunofluorescence microscopy with species-specific anti-HSP27 antibodies was performed to visualize the intracellular distribution of Chinese hamster HSP27 in *neo* cells (clone 3) (A and D), human HSP27 in HU27 cells (clone 6) (B and E), and mutant human HSP27 in HU27pm3 cells (clone V) (C and F) before (A to C) and after (D to F) heat shock at 44°C for 1.5 h. The pictures represent thin optical sections (confocal microscopy) made at different levels in the cells: (A to C) sections near the cell cortex at the apical face of the cells; (D to F) sections near the center of the cells to illustrate the localization of HSP27 in perinuclear structures following heat shock. Bar, 10 μm.

tion of HSP27, as obtained after arsenite treatment, yielded a single major band in the range of 125 kDa, whereas discrete intermediate species (200 to 150 kDa) were obtained following heat shock or mitogenic stimulation, which induces intermediate levels of phosphorylation. Treatments with cytochalasin D, which induced only a slight increase in HSP27 phosphorylation (Fig. 5D), produced a partial but reproducible and dose-dependent shift toward a species of 200 kDa (Fig. 9, lanes 10 and 11). Human HSP27 in HeLa cells behaved essentially as the Chinese hamster protein. It was present as a major complex of ca. 250 kDa that was reduced to 125 kDa after treatment with arsenite (lanes 13 and 14). After cytochalasin D treatment, a faint band became visible at 150 kDa (lanes 15 and 16).

Migration by pore exclusion limit electrophoresis was done until equilibrium and is not expected to be dependent on phosphorylation-induced changes in the charge of the proteins. To ascertain that HSP27 was migrating at equilibrium and that the position of HSP27 in the gels was strictly dependent on the size of the protein complexes, we performed several control experiments in which the time of migration (8 to 48 h) and the gradient of acrylamide (5 to 17% and 4 to 24%) were varied. Essentially the same results were obtained under all conditions (data not shown). Furthermore, HSP27 complexes were also analyzed on a size exclusion Superose 12 column (Fig. 10). Size exclusion chromatography yielded estimates of apparent molecular weight higher than those predicted from pore exclusion limit electrophoresis; nevertheless, the results were qualitatively similar. From a uniform apparent molecular mass of some 800 kDa, the Chinese hamster HSP27 particles were distributed in three peaks at about 800, 400, and 100 kDa after phosphorylation induced by arsenite treatments (Fig. 10).

To ascertain that the changes in the HSP27 oligomeric structure occurred as a consequence of phosphorylation rather than

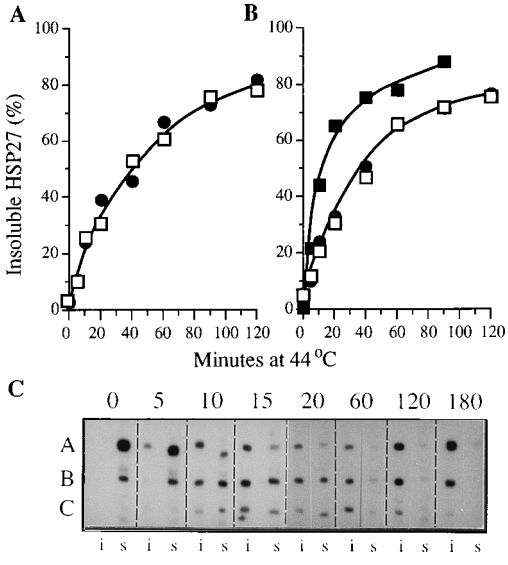

FIG. 7. Heat shock-induced insolubilization of wild-type and mutant HSP27. At various times during continuous treatment at 44°C, cells were lysed in hypotonic buffer containing 0.5% Triton X-100. (A and B) Kinetics of insolubilization. Total proteins from equal portions of the soluble and insoluble fractions were run on 1-D SDS-PAGE gels, and the proportion of HSP27 in each fraction was evaluated on immunoblots with species-specific antisera against the human (A) or Chinese hamster (B) HSP27. Symbols: ■, CCL39 cells; ●, HU27 (clone 6) cells; □, HU27pm3 (clone V) cells. (C) Distribution of the HSP27 isoforms in the Triton-soluble and the Triton-insoluble fractions. Equal portions of the soluble (s) and insoluble (i) fractions obtained from control untransfected CCL39 clonal cells were analyzed by IEF-PAGE. Chinese hamster HSP27 isoforms A, B, and C were detected immunologically with a specific antibody against hamster HSP27.

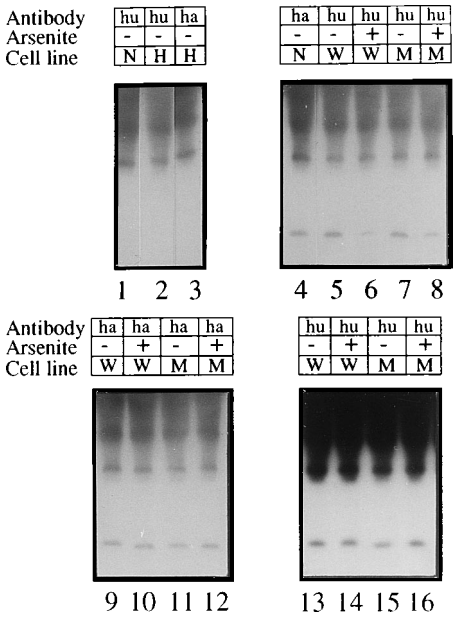

FIG. 8. Coimmunoprecipitation of endogenous Chinese hamster HSP27 and exogenous human HSP27 (wild type and mutant) in CCL39 transfected cells. Nondenaturing immunoprecipitation analysis was performed in control and arsenite-treated (200 μM, 1 h) *neo* (clone 3) (N), HU27 (clone 6) (W), and HU27pm3 (clone V) (M) cell lines with either anti-Chinese hamster HSP27 (ha) or anti-human HSP27 (hu) antibodies. Equal amounts of immunoprecipitates were run on SDS-PAGE gels under nonreducing conditions, and endogenous Chinese hamster HSP27 (lanes 1 to 12) or exogenous human HSP27 (lanes 13 to 16) present in each immunoprecipitate were immunologically detected with the anti-Chinese hamster HSP27 or anti-human HSP27 antibodies, respectively. Appropriate control samples of *neo* (clone 3) (N) and HeLa (H) cells were tested to verify the specificity of the antibodies (lanes 1 to 3). The relative amounts of Chinese hamster HSP27 immunoprecipitated under the various conditions as determined by densitometry are 0, 0, 0, 1, 1.1, 0.3, 0.8, 0.3, 0.9, 0.9, 0.7, and 0.8 in lanes 1 to 12, respectively. The relative amounts of human HSP27 in lane 14 versus lane 13 and in lane 16 versus lane 15 are 0.95 and 1.2, respectively. The smear at the top of the gels corresponds to unreduced high-molecular-weight immunoglobulin G.

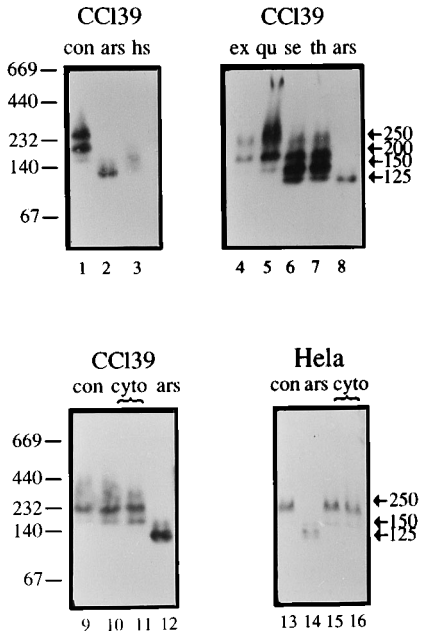

FIG. 9. Phosphorylation-induced changes in the oligomeric size of HSP27 structures in Chinese hamster CCL39 or human HeLa cells. Protein extracts were prepared from control exponentially growing cells left untreated (con, ex) or exposed to heat shock (20 min at 44°C) (hs), arsenite (200 μM for 1 h) (ars), or cytochalasin D (0.5 μM [lanes 10 and 15] or 2.5 μM [lanes 11 and 16] for 1 h) (cyto) or from quiescent cells before (qu) or after stimulation with serum (10% for 15 min) (se) or thrombin (1 U/ml for 15 min) (th). After fractionation by pore exclusion limit electrophoresis on nondenaturing polyacrylamide gels, HSP27 was detected with species-specific antisera against Chinese hamster (lanes 1 to 12) or human (lanes 13 to 16) HSP27. The numbers on the left indicate the positions of the molecular mass markers (thyroglobulin, 669 kDa; ferritin, 440 kDa; catalase, 232 kDa; lactate dehydrogenase, 140 kDa; albumin, 67 kDa). The arrows indicate the apparent molecular weights of the major HSP27 species.

through other modifications induced in cells by these agents, pore exclusion limit electrophoresis analyses were done with extracts of Chinese hamster cells expressing the wild-type or the nonphosphorylatable human HSP27. After fractionation, the extracts were probed with both Hu27Ab and anti-Ha (L2R3) antibodies. In both unstressed and stressed or stimulated cells, wild-type human HSP27 and endogenous Chinese hamster HSP27 behaved similarly to each other and to HSP27 from untransfected cells (Fig. 11). The two proteins comigrated under all conditions as species of identical molecular weights, in agreement with their ability to be coimmunoprecipitated. Furthermore, as was found with pure Chinese hamster HSP27 particles, the heterologous structures were also reduced in size after stress or stimulation. These results explained the reduced efficiency of coimmunoprecipitation found under such conditions, since, assuming a random association of the proteins in the oligomers, a reduced size is expected to increase the probability of formation of homotypic particles. It is notable that the pattern of distribution of the structures was more diffuse in cells expressing both human and Chinese hamster HSP27 than in CCL39 or HeLa cells. This can be explained by the formation of random heterotypic structures containing different numbers of human and Chinese hamster HSP27 which differ in molecular mass by ~2 kDa.

The redistribution of human HSP27 oligomers to lower-molecular-weight species was strongly inhibited in cells expressing the mutant protein. Interestingly, however, most of the endogenous Chinese hamster HSP27 species in those cells, although initially associated with the human protein (as evidenced by their coimmunoprecipitation and comigration in the gels), shifted to lower-molecular-weight species when phosphorylation was induced. These results implied that the HSP27 particles are highly dynamic: phosphorylated Chinese hamster proteins released from the larger structures rapidly reoligomerize into smaller structures, whereas the nonphosphorylated human proteins appear to reassociate spontaneously into larger particles. No monomeric or dimeric intermediates were ever detected.

DISCUSSION

A direct correlation was found between the cell thermosensitivity and the level of the protein in stable Chinese hamster clones constitutively expressing the human HSP27. The levels of expression of total HSP27 (Chinese hamster and human) expressed in the transfected clones used in this study were well below the level of HSP27 found after heat shock of these cells, meaning that HSP27 exerts a protective function at physiologically relevant concentrations. Intriguingly, cells expressing equivalent and even larger amounts of nonphosphorylatable HSP27 were only slightly protected compared with control cells. We conclude that phosphorylation of HSP27, which occurs during the first minutes of heat shock, is essential for activating most of the protective function of HSP27.

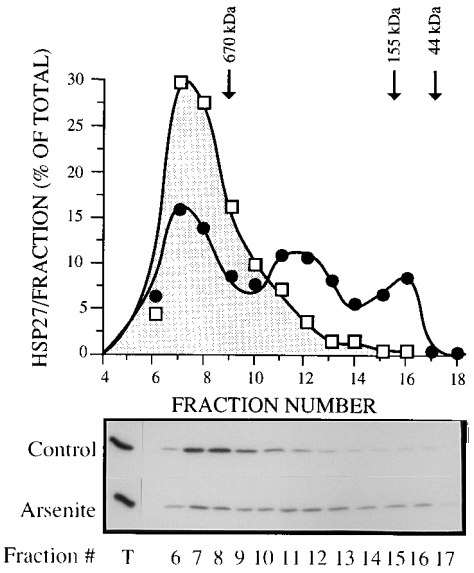

FIG. 10. Superose 12 chromatography of HSP27 from control and arsenite-treated CCL39 *neo* cells. Cell extracts were prepared by nonionic-detergent lysis and fractionated on a Superose 12 sizing column. Fractions were analyzed on SDS-PAGE gels, and HSP27 was immunologically detected following electroblotting. The relative amount of Chinese hamster HSP27 present in each fraction was determined by densitometric scanning of the autoradiograms and is expressed above the autoradiogram as the percentage of total HSP27 per fraction. Symbols: □, control untreated CCL39 *neo* cells; ●, arsenite-treated CCL39-neo cells; T, total unfractionated sample. Molecular mass markers: thyroglobulin, 670 kDa; gamma globulin, 155 kDa; ovalbumin, 44 kDa.

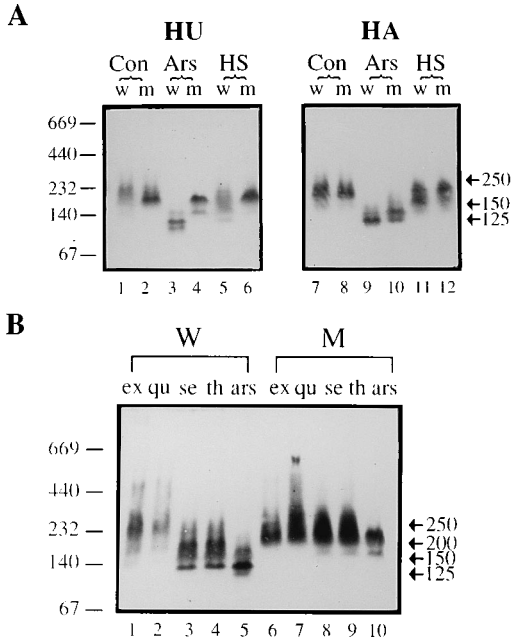

FIG. 11. Induced changes in the supramolecular structure of HSP27 are dependent on phosphorylation. Cells overexpressing either the wild-type human HSP27 (W, w) or the nonphosphorylatable human HSP27 (M, m) were lysed in nonionic-detergent buffer immediately after treatment with phosphorylation inducers. Cell extracts were analyzed by pore exclusion limit electrophoresis. (A) Cells were left untreated (Con), heat shocked (44°C for 20 min) (HS), or treated with arsenite (200 μM for 1 h) (Ars), and HSP27 species were detected, following denaturation and electroblotting, with specific antisera against Chinese hamster HSP27 (HA) or human HSP27 (HU). For heat-shocked extracts, twice as much material has been put on the gel to correct for the loss caused by heat-induced insolubilization of the protein. (B) Exponentially growing cells were left untreated (ex), arsenite treated (ars), serum starved for 24 h (qu), or serum starved for 24 h and then stimulated for 15 min with 10% fetal calf serum (se) or 1 U of thrombin per ml (th). Human HSP27 was detected with Hu27Ab.

An evaluation of several independent parameters confirmed that the protein structure was not severely altered by the Ser → Gly substitutions and that the lack of phosphorylation alone was responsible for the diminished function. We found that, in the numerous clonal cell lines evaluated, the mutated proteins were expressed at levels equivalent to those of the wild-type proteins, suggesting that the two types of proteins had equal stabilities. This was also indicated by the identical solubilities of the two proteins. We also found that the mutant proteins had a general cytoplasmic distribution and enhanced expression in membrane protrusions identical to the wild-type proteins. Most importantly, the mutant HSP27 retained the ability to interact with itself or with the endogenous Chinese hamster protein and to form oligomeric structures of a size similar to wild-type human HSP27. Furthermore, we found no evidence that the expression of the proteins (wild type or mutant) was inducing a stress response in the recipient cells. This was evaluated carefully for all clonal cell lines, either individually or in pools, by monitoring the levels of two other heat shock proteins, HSP68 and HSP70, both before and after heat shock and by measuring the phosphorylation response of the endogenous HSP27. In all cell lines, endogenous HSP27, HSP68, and HSP70 were expressed at normal levels both before (Fig. 2D) and after (data not shown) heat shock, and phosphorylation of endogenous HSP27, which is highly sensitive to stress, was not modified. Nevertheless, a small stress response generated by the presence of the mutant protein cannot be totally excluded and may explain the small increase in thermal resistance observed in cells expressing the nonphosphorylatable protein. An alternative explanation is that HSP27 also has a phosphorylation-independent function. At the physiological concentrations of the proteins investigated here, this function must play a minor role in the overall resistance provided by wild-type HSP27.

We looked at several properties of HSP27 that are known to be modified by heat shock and thus could be mediated by phosphorylation and be involved in modulating the function of HSP27. Several studies have reported that heat shock causes insolubilization and relocalization of mammalian HSP27 to or around the nucleus (for a review, see reference 4). The functional significance of these effects remained unclear. In this study, we found no difference in the kinetics of translocation or insolubilization of the nonphosphorylatable versus the wild-type HSP27. Moreover, no systematic enrichment of phosphorylated species in either the soluble or insoluble fractions was detected after continuous heat shock in control cells. It thus appears unlikely that these modifications in HSP27 properties are mediated by phosphorylation. Since phosphorylation was required for full activation of HSP27 protective functions but was dispensable for insolubilization and relocalization of the protein, these changing properties of HSP27 may not be involved or at least are not sufficient in thermoprotection. It is conceivable that the insolubilization and translocation of HSP27 during heat shock simply reflect the protein denaturing effect of heat. A large number of other proteins are similarly insolubilized and associate with nuclear structures during heat shock (13, 23, 24, 33, 45, 54).

In contrast, we obtained evidence that all the inducers of HSP27 phosphorylation that we investigated induced major changes in the oligomeric structure of the protein. All members of the small heat shock protein/α-crystallin family so far examined, including those from yeast, chicken, *Drosophila*, and

human cells, have been found to form oligomeric structures that display native molecular masses on sizing columns between 300 and >1,000 kDa (3–8, 10, 47, 51, 53). Depending on the fractionation procedure used, HSP27 from unstressed exponentially growing Chinese hamster cells was found to behave as a protein of ~800 kDa on a Superose 12 column, which is in agreement with previous analyses by similar sizing techniques, or as a doublet of ~250 and 200 kDa on native polyacrylamide gels. The reason for the difference in size obtained by the two fractionation techniques has not been investigated in detail and remains unclear. More studies are required to determine the actual size of HSP27 in situ. Nevertheless, it is likely that the changes observed in both cases after phosphorylation reflect a real change in the structures or the stability of the HSP27 oligomers. By both fractionation procedures, we found that phosphorylation causes a dramatic decrease in the size of the oligomers. The higher resolving properties of electrophoresis revealed, at intermediate phosphorylation levels, a ladder-like distribution of oligomers with size differing by 25 to 50 kDa in the 125- to 250-kDa range. When HSP27 was maximally phosphorylated, a unique species of approximately 125 kDa was found to accumulate.

As has been proposed for the α-crystallin oligomer, HSP27 may be organized in a multilayer structure composed of a central stable core of some 125 kDa (four to six subunits), corresponding to the smallest oligomer that we detected, to which additional HSP27 molecules (monomers or dimers to accommodate the 25- to 50-kDa difference observed between the various species) are bound with a strength that is modulated by phosphorylation. As phosphorylation is increased, some subunits are released and probably promptly reassociate in the core structure, since we could not observe particles smaller than 125 kDa.

Mitogenic stimulation and stress induce the same HSP27 kinase, the phosphorylation of HSP27 at the same sites (19, 31), and similar phosphorylation-dependent modifications in the oligomeric structure of the protein. It is thus likely that the role of HSP27 in stress protection is related to its function during mitogenic stimulation. In quiescent fibroblasts stimulated by addition of mitogens, HSP27 enhances accumulation of F-actin, whereas the nonphosphorylatable HSP27 inhibits the initial accumulation of filaments (36). Similarly, we found in the present work that the presence of elevated levels of HSP27 modifies the kinetics of reaccumulation of actin filaments in cells recovering from severe disruption of the microfilaments after cytochalasin D treatments. Accumulation of F-actin during the recovery period was enhanced in the presence of the phosphorylatable HSP27, whereas mutant HSP27 produced no such enhancement. As a possible consequence of these contrasting phosphorylation-dependent effects of HSP27 on actin dynamics, cells expressing wild-type HSP27 were found to be highly resistant to cytochalasin D treatments, whereas cells expressing the nonphosphorylatable HSP27 appeared to be as sensitive as the control cells. Recent in vitro observations also supported a role of phosphorylation in modulating the activities of HSP27 at the actin level. Benndorf et al. (9) confirmed the observations of Miron et al. (41, 42) that HSP27 can inhibit actin polymerization in vitro and found that this inhibiting activity was highly reduced by phosphorylation. From these results and those reported in the present study, it is conceivable that in vivo, unphosphorylated HSP27 similarly binds to the barbed ends of microfilaments, limiting the rate of actin polymerization. Upon mitogenic stimulation, heat shock, and other toxic treatments, changes in the quaternary structure of the protein, induced by local phosphorylation of cortical HSP27, may reduce the binding affinity of HSP27, resulting in a higher rate of actin monomer addition. Because HSP27 is not the only protein involved in the control of actin polymerization (1, 2, 52, 55), a higher concentration of HSP27 in cells would increase the proportion of HSP27 relative to other actin-capping proteins, enhancing the polymerization rate in response to inducers of HSP27 phosphorylation. As a result, the rate of F-actin disruption would be reduced in HSP27-overexpressing cells during stress and the rate of accumulation of F-actin would be enhanced during mitogenic stimulation. In contrast, the presence of large amounts of the nonphosphorylatable HSP27 would increase the life time of HSP27 at the barbed end and reduce the polymerization rate of actin. This would render actin filaments more sensitive to stress-induced destruction and less responsive to mitogenic stimulation. Stabilization of microfilaments may thus be an important contributing factor to HSP27-mediated stress resistance. Since the action of heat shock on microfilaments constitutes only one of the multiple alterations that may disrupt cellular homeostasis and cause cell death, the level of protection afforded by HSP27 probably represents the contribution of microfilament stabilization to overall survival.

While our manuscript was being finalized for submission, a number of papers were published suggesting, in agreement with the results presented in this paper, a modulation of the structure and function of HSP27 by phosphorylation. Mehlen and Arrigo (38) suggested a correlation between changes in the oligomeric structure of HSP27 and phosphorylation induced by serum. Similarly, Kato et al. (25) found a reduction in the size of HSP27 species measured on sucrose gradients upon phosphorylation by heat shock or exposures to a variety of agents. Finally, as mentioned above, Benndorf et al. (9) found that the phosphorylation and oligomeric status of HSP27 influenced its ability to block actin polymerization in vitro. However, Knauf et al. (26) reported that overexpression of a phosphorylation mutant of mouse HSP27 (hsp25) was as efficient as the wild-type protein in protecting cells from heat shock-induced cell death in a transient-transfection system and that in vitro phosphorylation of recombinant HSP27 has no effect on its oligomeric structure. The reason for the almost complete disagreement between this and results from other laboratories is unclear.

ACKNOWLEDGMENTS

We thank Alain Guimond for performing the initial fractionation of HSP27 oligomers on native gels, Claude Chamberland for assistance with confocal microscopy, and Robert Tanguay and Andrei Laszlo for providing anti-HU71 and anti-HSP70 antibodies, respectively.

This work was supported by grants MT-1088 from the Medical Research Council of Canada (to J.L.) and GM 43167 from the National Institutes of Health (to L.A.W. and E.H.). J.N.L. was supported by a studentship from the Medical Research Council of Canada.

REFERENCES

1. **Aderem, A.** 1992. Signal transduction and the actin cytoskeleton: the roles of MARCKS and profilin. Trends Biochem. Sci. **17:**438–443.
2. **Arpin, M., M. Algrain, and D. Louvard.** 1994. Membrane-actin microfilament connections: an increasing diversity of players related to band 4.1. Curr. Opin. Cell Biol. **6:**136–141.
3. **Arrigo, A. P.** 1987. Cellular localization of HSP23 during Drosophila development and following subsequent heat shock. Dev. Biol. **122:**39–48.
4. **Arrigo, A. P., and J. Landry.** 1994. Expression and function of the low-molecular-weight heat shock proteins, p. 335–373. *In* R. I. Morimoto, A. Tissières, and C. Georgopoulos (ed.), The biology of heat shock proteins and molecular chaperones. Cold Spring Harbor Laboratory Press, Cold Spring Harbor, N.Y.
5. **Arrigo, A. P., J. P. Suhan, and W. J. Welch.** 1988. Dynamic changes in the structure and intracellular locale of the mammalian low-molecular-weight heat shock protein. Mol. Cell. Biol. **8:**5059–5071.
6. **Arrigo, A. P., and W. J. Welch.** 1987. Characterization and purification of the

small 28,000-dalton mammalian heat shock protein. J. Biol. Chem. **262:** 15359–15369.
7. **Augusteyn, R. C., and J. F. Koretz.** 1987. A possible structure for alpha-crystallin. FEBS Lett. **222:**1–5.
8. **Behlke, J., G. Lutsch, M. Gaestel, and H. Bielka.** 1991. Supramolecular structure of the recombinant murine small heat shock protein hsp25. FEBS Lett. **288:**119–122.
9. **Benndorf, R., K. Hayes, S. Ryazantsev, M. Wieske, J. Behlke, and G. Lutsch.** 1994. Phosphorylation and supramolecular organization of murine small heat shock protein HSP25 abolish its actin polymerization-inhibiting activity. J. Biol. Chem. **269:**20780–20784.
10. **Bentley, N. J., I. T. Fitch, and M. F. Tuite.** 1992. The small heat-shock protein Hsp26 of Saccharomyces cerevisiae assembles into a high molecular weight aggregate. Yeast **8:**95–106.
11. **Chambard, J.-C., A. Franchi, A. Le Cam, and J. Pouysségur.** 1983. Growth factor-stimulated protein phosphorylation in G0/G1-arrested fibroblasts. Two distinct classes of growth factors with potentiating effects. J. Biol. Chem. **258:**1706–1713.
12. **Clos, J., J. T. Westwood, P. B. Becker, S. Wilson, K. Lambert, and C. Wu.** 1990. Molecular cloning and expression of a hexameric Drosophila heat shock factor subject to negative regulation. Cell **63:**1085–1097.
13. **Dubois, M. F., A. G. Hovanessian, and O. Bensaude.** 1991. Heat-shock-induced denaturation of proteins. Characterization of the insolubilization of the interferon-induced p68 kinase. J. Biol. Chem. **266:**9707–9711.
14. **Gabai, V. L., and A. E. Kabakov.** 1993. Tumor cell resistance to energy deprivation and hyperthermia can be determined by the actin skeleton stability. Cancer Lett. **70:**25–31.
15. **Gaestel, M., W. Schroder, R. Benndorf, C. Lippmann, K. Buchner, F. Hucho, V. A. Erdmann, and H. Bielka.** 1991. Identification of the phosphorylation sites of the murine small heat shock protein hsp25. J. Biol. Chem. **266:**14721–14724.
16. **Glass, J. R., R. G. DeWitt, and A. E. Cress.** 1985. Rapid loss of stress fibers in Chinese hamster ovary cells after hyperthermia. Cancer Res. **45:**258–262.
17. **Gorman, C., R. Padmanabhan, and B. H. Howara.** 1983. High efficiency DNA-mediated transformation of primate cells. Science **221:**551–553.
18. **Hickey, E., S. E. Brandon, R. Potter, G. Stein, J. Stein, and L. A. Weber.** 1986. Sequence and organization of genes encoding the human 27 kDa heat shock protein. Nucleic Acids Res. **14:**4127–4145.
19. **Huot, J., H. Lambert, F. Houle, J. N. Lavoie, and J. Landry.** Identification and characterization of p45-54 HSP27-kinase, a stress-sensitive kinase which may activate the phosphorylation-dependent protective function of mammalian heat shock protein 27. Eur. J. Biochem., in press.
20. **Iida, K., H. Iida, and I. Yahara.** 1986. Heat shock induction of intranuclear actin rods in cultured mammalian cells. Exp. Cell Res. **165:**207–215.
21. **Iwaki, T., A. Iwaki, J. Tateishi, and J. E. Goldman.** 1994. Sense and antisense modification of glial αB-crystallin production results in alterations of stress fiber formation and thermoresistance. J. Cell Biol. **125:**1385–1393.
22. **Jakob, U., M. Gaestel, K. Engel, and J. Buchner.** 1993. Small heat shock proteins are molecular chaperones. J. Biol. Chem. **268:**1517–1520.
23. **Kampinga, H. H.** 1993. Thermotolerance in mammalian cells. Protein denaturation and aggregation, and stress proteins. J. Cell Sci. **104:**11–17.
24. **Kampinga, H. H., J. G. Luppes, and A. W. Konings.** 1987. Heat-induced nuclear protein binding and its relation to thermal cytotoxicity. Int. J. Hyperthermia **3:**459–465.
25. **Kato, K., K. Hasgawa, S. Goto, and Y. Inaguma.** 1994. Dissociation as a result of phosphorylation of an aggregated form of the small stress protein hsp27. J. Biol. Chem. **269:**11274–11278.
26. **Knauf, U., U. Jakob, K. Engel, J. Buchner, and M. Gaestel.** 1994. Stress- and mitogen-induced phosphorylation of the small heat shock protein Hsp25 by MAPKAP kinase 2 is not essential for chaperone properties and cellular thermoresistance. EMBO J. **13:**54–60.
27. **Kolega, J., L. W. Janson, and D. L. Taylor.** 1991. The role of solation-contraction coupling in regulating stress fiber dynamics in nonmuscle cells. J. Cell Biol. **114:**993–1003.
28. **Landry, J., D. Bernier, P. Chrétien, L. M. Nicole, R. M. Tanguay, and N. Marceau.** 1982. Synthesis and degradation of heat shock proteins during development and decay of thermotolerance. Cancer Res. **42:**2457–2461.
29. **Landry, J., P. Chrétien, H. Lambert, E. Hickey, and L. A. Weber.** 1989. Heat shock resistance conferred by expression of the human HSP27 gene in rodent cells. J. Cell Biol. **109:**7–15.
30. **Landry, J., P. Chrétien, A. Laszlo, and H. Lambert.** 1991. Phosphorylation of HSP27 during development and decay of thermotolerance in Chinese hamster cells. J. Cell. Physiol. **147:**93–101.
31. **Landry, J., H. Lambert, M. Zhou, J. N. Lavoie, E. Hickey, L. A. Weber, and C. W. Anderson.** 1992. Human HSP27 is phosphorylated at serines 78 and 82 by heat shock and mitogen-activated kinases that recognize the same amino acid motif as S6 kinase II. J. Biol. Chem. **267:**794–803.
32. **Laszlo, A.** 1992. The effects of hyperthermia on mammalian cell structure and function. Cell Prolif. **25:**59–87.
33. **Laszlo, A., W. Wright, and J. L. Roti Roti.** 1992. Initial characterization of heat-induced excess nuclear proteins in HeLa cells. J. Cell. Physiol. **151:**519–532.
34. **Lavoie, J., P. Chrétien, and J. Landry.** 1990. Sequence of the Chinese hamster small heat shock protein HSP27. Nucleic Acids Res. **18:**1637.
35. **Lavoie, J. N., G. Gingras-Breton, R. M. Tanguay, and J. Landry.** 1993. Induction of Chinese hamster HSP27 gene expression in mouse cells confers resistance to heat shock. HSP27 stabilization of the microfilament organization. J. Biol. Chem. **268:**3420–3429.
36. **Lavoie, J. N., E. Hickey, L. A. Weber, and J. Landry.** 1993. Modulation of actin microfilament dynamics and fluid phase pinocytosis by phosphorylation of heat shock protein 27. J. Biol. Chem. **268:**24210–24214.
37. **Li, G. C., and Z. Werb.** 1982. Correlation between synthesis of heat shock proteins and development of thermotolerance in Chinese hamster fibroblasts. Proc. Natl. Acad. Sci. USA **79:**3218–3222.
38. **Mehlen, P., and A. P. Arrigo.** 1994. The serum-induced phosphorylation of mammalian hsp27 correlates with changes in its intracellular localization and levels of oligomerization. Eur. J. Biochem. **221:**327–334.
39. **Merck, K. B., P. J. Groenen, C. E. Voorter, W. A. de Haard-Hoekman, J. Horwindal, and W. W. de Jong.** 1993. Structural and functional similarities of bovine alpha-crystallin and mouse small heat-shock protein. A family of chaperones. J. Biol. Chem. **268:**1046–1052.
40. **Mirabelli, F., A. Salis, V. Marinoni, G. Finardi, G. Bellomo, H. Thor, and S. Orrenius.** 1988. Menadione-induced bleb formation in hepatocytes is associated with the oxidation of thiol groups in actin. Arch. Biochem. Biophys. **264:**261–269.
41. **Miron, T., K. Vancompernolle, J. Vandekerckhove, M. Wilchek, and B. Geiger.** 1991. A 25-kD inhibitor of actin polymerization is a low molecular mass heat shock protein. J. Cell Biol. **114:**255–261.
42. **Miron, T., M. Wilchek, and B. Geiger.** 1988. Characterization of an inhibitor of actin polymerization in vinculin-rich fraction of turkey gizzard smooth muscle. Eur. J. Biochem. **178:**543–553.
43. **Ohtsuka, K., K. Tanabe, H. Nakamura, and C. Sato.** 1986. Possible cytoskeletal association of 69,000- and 68,000-dalton heat shock proteins and structural relations among heat shock proteins in murine mastocytoma cells. Radiat. Res. **108:**34–42.
44. **Parsell, D. A., and S. Lindquist.** 1994. Heat-shock protein and stress tolerance, p. 457–494. *In* R. I. Morimoto, A. Tissières, and C. Georgopoulos (ed.), The biology of heat shock proteins and molecular chaperones. Cold Spring Harbor Laboratory Press, Cold Spring Harbor, N.Y.
45. **Pinto, M., M. Morange, and O. Bensaude.** 1991. Denaturation of proteins during heat shock. In vivo recovery of solubility and activity of reporter enzymes. J. Biol. Chem. **266:**13941–13946.
46. **Sampath, P., and T. D. Pollard.** 1991. Effects of cytochalasin, phalloidin, and pH on the elongation of actin filaments. Biochemistry **30:**1973–1980.
47. **Siezen, R. J., J. G. Bindels, and H. J. Hoenders.** 1980. The quaternary structure of bovine alpha-crystallin. Effects of variation in alkaline pH, ionic strength, temperature and calcium ion concentration. Eur. J. Biochem. **111:** 435–444.
48. **St-Amand, J.** 1994. M.Sc. thesis. Université Laval, Québec, Québec, Canada.
49. **Subjeck, J. R., and J. J. Sciandra.** 1982. Co-expression of thermotolerance and heat-shock proteins in mammalian cells, p. 405–411. *In* M. J. Schlesinger, M. J. Ashburner, and A. Tissières (ed.), Heat shock: from bacteria to man. Cold Spring Harbor Laboratory Press, Cold Spring Harbor, N.Y.
50. **Tanguay, R. M., Y. Wu, and E. W. Khandjian.** 1993. Tissue-specific expression of heat shock proteins of the mouse in the absence of stress. Dev. Genet. **14:**112–118.
51. **Tardieu, A., D. Laporte, P. Licino, B. Krop, and M. Delaye.** 1986. Calf lens alpha-crystallin quaternary structure. A three-layer tetrahedral model. J. Mol. Biol. **192:**711–724.
52. **Theriot, J. A., and T. J. Mitchison.** 1993. The three faces of profilin. Cell **75:**835–838.
53. **Walsh, M. T., A. C. Sen, and B. Chakrabarti.** 1991. Micellar subunit assembly in a three-layer model of oligomeric alpha-crystallin. J. Biol. Chem. **266:**20079–20084.
54. **Warters, R. L., L. M. Brizgys, R. Sharma, and J. L. Roti Roti.** 1986. Heat shock (45 degrees C) results in an increase of nuclear matrix protein mass in HeLa cells. Int. J. Radiat. Biol. **50:**253–268.
55. **Weeds, A., and S. Maciver.** 1993. F-actin capping proteins. Curr. Opin. Cell Biol. **5:**63–69.
56. **Welch, W. J., and J. P. Suhan.** 1985. Morphological study of the mammalian stress response: characterization of changes in cytoplasmic organelles, cytoskeleton, and nucleoli, and appearance of intranuclear actin filaments in rat fibroblasts after heat-shock treatment. J. Cell Biol. **101:**1198–1211.
57. **Zhou, M., H. Lambert, and J. Landry.** 1993. Transient activation of a distinct serine protein kinase is responsible for 27-kDa heat shock protein phosphorylation in mitogen-stimulated and heat-shocked cells. J. Biol. Chem. **268:**35–43.

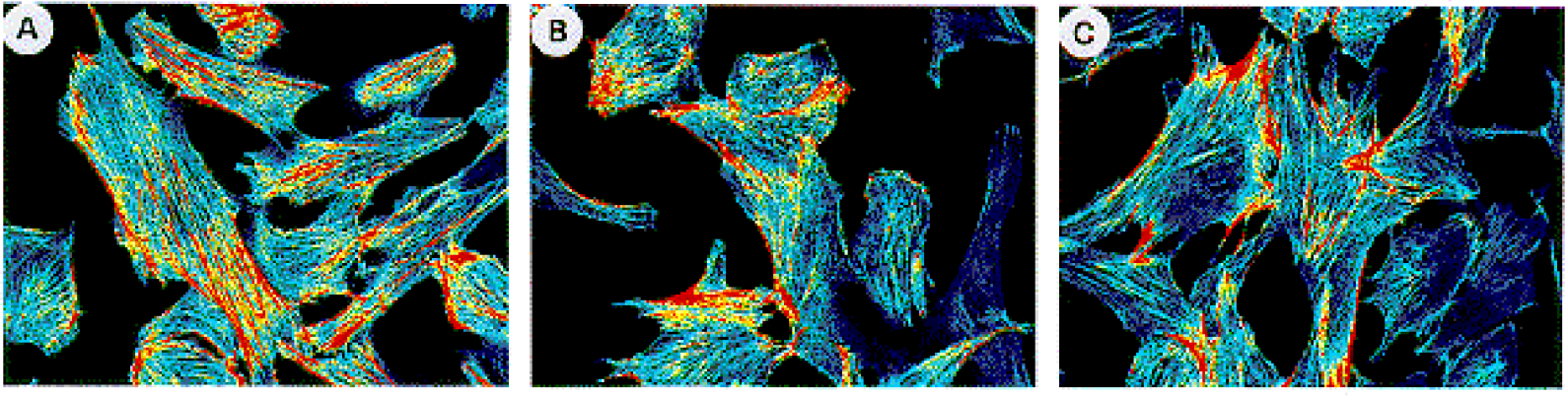
A
B
C

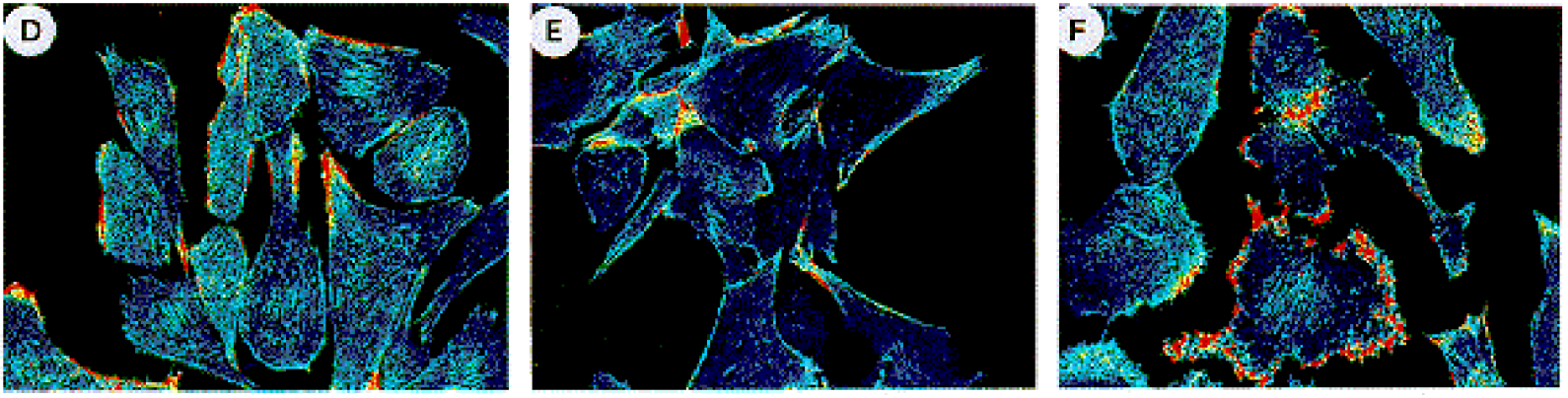
D
E
F

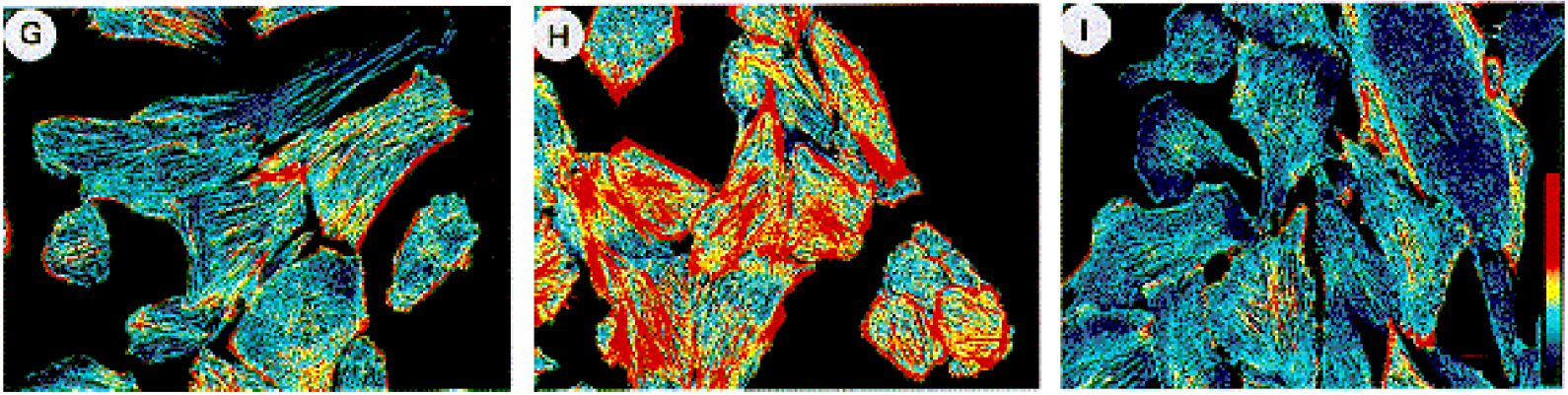
G
H
I